ARTICLE　　　　　　　　　　　　　　　　　　　　　**Open Access**

Functional tissue-engineered bone-like graft made of a fibrin scaffold and TG2 gene-modified EMSCs for bone defect repair

Wentao Shi[1,2,3], Yunduan Que[1], Xuan Zhang[4], Lu Bian[1,3], Xuejian Yu[4], Xue Tang[4], Guofeng Yang[4], Yao Dai[2], Shiqi Bi[2], Demin Lv[2], Yuyan Weng[5], Weijiang Wu[2], Zhijian Zhang[2], Xiaojie Lu[3] and Naiyan Lu[4]

Abstract

The transplantation of tissue-engineered scaffolds with stem cells is a promising therapeutic approach for bone defect repair. To improve the therapeutic efficacy of this approach, in this study, a novel biofunctional live tissue-engineered bone-like graft was designed and constructed using a fibrin scaffold loaded with TG2 gene-modified ectomesenchymal stem cells (TG2-EMSCs) derived from nasal respiratory mucosa for bone defect repair. Autocalcification of the cell-free fibrin gel in osteogenic medium with additional alkaline phosphatase (ALP) and the osteogenic differentiation of TG2-EMSCs on the fibrin scaffold were assessed in vitro. The results indicated that the cell-free fibrin gel could autocalcify in the osteogenic medium with ALP and that the overexpression of TG2 by TG2-EMSCs could promote the osteogenic differentiation of these stem cells in the fibrin scaffold. Moreover, TG2 could enhance the deposition of extracellular matrix proteins in the fibrin scaffold, followed by calcification of the bone matrix in vitro. After transplantation into critical-sized cranial defects in rats, the functional tissue-engineered bone-like grafts improved bone regeneration. These results indicate that this tissue-engineered bone-like graft could improve the process of bone defect repair.

Introduction

The repair of large bone defects in orthopedics is a significant problem faced by orthopedic surgeons[1]. Common causes of bone defects include acute bone injuries, benign tumors, malignant tumors, bone infections, and fracture nonunion. The use of autologous bone grafts is considered the gold standard therapy for bone defects[2]. However, this treatment generally requires two operations, which not only increases the probability of infection but may also cause deformity, pain, or even functional problems. These drawbacks of autologous bone grafts encourage the development of improved strategies for bone defect repair. The transplantation of autologous stem cells and tissue-engineered bone-like grafts may offer a novel therapeutic approach for bone defect repair[3,4].

Bone defect repair and reconstruction are dynamic processes in which osteoblasts play a critical role because these cells are responsible for matrix production and osteoid mineralization[5]. Thus, one promising therapeutic approach is the transplantation of stem cells that can directly differentiate into osteoblasts. The bone marrow has been shown to contain a population of mesenchymal stem cells (BMSCs) with osteogenic potential[6]. However, the number of BMSCs that can be harvested is too low to meet the requirements for transplantation. In addition, the harvesting procedure is painful for the donor and may lead to bone marrow infection. Therefore, more ideal autologous stem cells are needed for the repair of bone defects. Previous studies conducted in our laboratory have

Correspondence: Naiyan Lu (lunaiyan@jiangnan.edu.cn)
[1]Nanjing Gaochun People's Hospital, 211300 Nanjing, People's Republic of China
[2]School of Medicine, Jiangsu University, 212001 Zhenjiang, Jiangsu Province, People's Republic of China
Full list of author information is available at the end of the article
These authors contributed equally: Wentao Shi, Yunduan Que, Xuan Zhang

shown that the lamina propria of the mucosa lining the respiratory region of the nasal cavity contains neural crest-derived ectomesenchymal stem cells (EMSCs), which can differentiate toward ectoderm and mesoderm lineages[7,8]. Moreover, EMSCs can be noninvasively and easily harvested from the respiratory region of the nasal cavity in adults, avoiding donor discomfort and pain. Given these favorable properties, strategies using autologous EMSCs may be better accepted by patients.

Our previous study revealed that EMSCs could strongly proliferate for over ten passages to meet the requirements for transplantation[8]. The amplified cells maintained strong vitality and produced extracellular matrix (ECM) proteins and cell growth factors. The EMSCs could be applied as a novel live biomaterial for the construction of an "all-in-one" niche for the differentiation of stem cells[7]. Most importantly, the EMSCs could be induced to differentiate into osteoblasts when seeded on a fibrin scaffold[8]. However, for repairing bone defects, in addition to ideal seed stem cells, biomaterial scaffolds as carriers and substrates are needed for stem cell growth and should facilitate the adhesion, proliferation, and osteogenic differentiation of the seed cells; such scaffolds should be easy to mineralize and transform into 3D bone-like tissue, allowing osteogenesis, osteoinduction, and osteoconduction in vivo. Meanwhile, the resulting tissue-engineered bone-like graft should be inexpensive, readily available, and easy to produce and handle[9,10].

Fibrin scaffolds have several advantages over other synthetic scaffolds[11–13]. First, fibrin scaffolds provide an ideal substrate for cellular adhesion, proliferation, and differentiation due to the abundant arginine-glycine-aspartic acid (RGD) sequences in fibrin. Second, the proteins secreted by seed cells, including ECM/bone matrix proteins, such as fibronectin (FN), laminin (LN), collagen (COL), osteocalcin (OCN), and osteopontin (OPN), and growth factors, such as bone morphogenetic protein 2 (BMP-2) and vascular endothelial growth factor (VEGF), could be deposited into fibrin scaffolds by transglutaminase 2 (TG2) cross-linking. Third, fibrin scaffolds possess a sponge-like structure that facilitates vascularization and mineralization[14,15]. Finally, fibrin scaffolds possess ideal histological compatibility and can be reconstructed in vivo. However, rapid degradation of the native fibrin scaffold in vivo is disadvantageous for its application as a carrier of stem cells to directly repair large bone defects[16]. Therefore, prolonging the half-life and stabilizing the three-dimensional structure and subsequent mineralization of gel-like fibrin scaffolds in vitro and in vivo are necessary for the transplantation of tissue-engineered grafts to repair large bone defects. It is rational to design and construct a novel functional tissue-engineered bone-like graft made of TG2 gene-modified EMSCs and a fibrin scaffold for bone defect repair in the future.

TG2 is a member of the transglutaminase family that transamidates and cross-links proteins[17]. The majority of the cellular TG2 pool is present in the cytoplasm, but TG2 is also found in the mitochondria and the nucleus, and some TG2 is localized extracellularly, including in the plasma membrane and ECM[18]. To the best of our knowledge, TG2 also serves important enzymatic and nonenzymatic functions. Secreted TG2 can cross-link various ECM proteins, such as FN, LN, COL, and OPN, and certain soluble growth factors, such as BMP-2 and VEGF[19]. Furthermore, TG2 regulates the interaction between the ECM and soluble growth factors through noncovalent interactions with integrins and growth factor receptors. Maria[20] identified highly active TG2 enzymes in intramembranous bone and osteoblast-like bone cells in vitro. In addition, current studies have shown that FXIII can stabilize fibrin scaffolds and reduce the degradation rate; FXIII belongs to the family of transglutaminases and serves the same cross-linking function as TG2[21–23]. Previous studies have demonstrated that TG2 activity is required for the formation of an FN–COL network, which is essential for further osteoblast differentiation, matrix production, and ultimately mineralization[24]. However, no studies have reported the role of TG2 in the differentiation of EMSCs into osteoblasts or the transplantation of TG2 gene-modified EMSCs for bone defect repair. The use of cell therapy combined with tissue engineering techniques to enhance the regeneration of injured tissues and organs has become one of the most active and effective strategies in trauma repair surgery. Adenoviruses will likely play an important role in paving the way for effective clinical gene therapy[25,26]. In this study, a novel functional tissue-engineered bone-like graft of TG2 gene-modified EMSCs and a fibrin scaffold was constructed, and the therapeutic efficacy of this graft in bone defect repair was evaluated in vivo.

Materials and methods
Reagents

Dulbecco's modified Eagle's medium/F12 (DMEM/F12, Gibco), fetal bovine serum (FBS, Gibco), penicillin/streptomycin, and trypsin were obtained from Invitrogen Corporation (Carlsbad, CA, USA). Vimentin, S100, and nestin primary antibodies were obtained from Santa Cruz (California, USA). Antibodies against TG2, COL I, OCN, OPN, LN, BMP-2, VEGF, and FN were purchased from Abcam (Cambridge, UK). The β-tubulin antibody was provided by Boster (Wuhan, Hubei, China). Alkaline phosphatase (ALP), dexamethasone, cystamine (CYS), L-ascorbic acid 2-phosphate, β-glycerophosphate, 1,25-dihydroxy vitamin D3, and alizarin red S were purchased from Sigma-Aldrich (St. Louis, MO, USA). Rat fibrinogen and thrombin were obtained from Sigma-Aldrich. Immunofluorescence-related secondary antibodies were

obtained from Sigma-Aldrich, and Western blotting-related secondary antibodies were provided by Boster (Wuhan, China). Nattokinase was obtained from Wake Pure Chemical Industries (Wako Ltd, Japan). Ad-TG2-GFP and Ad-GFP adenoviruses were constructed by Nanjing GenScript Bioengineering Technology and Services Co., Ltd (Nanjing, China)

Isolation and identification of EMSCs

Male Sprague–Dawley (SD) rats were obtained from the Jiangsu University Experimental Animal Center. The animal experimental protocols were approved by Jiangsu University. The rats were deeply anesthetized by an intraperitoneal injection of phenobarbital sodium (200 mg/kg). Tissue-adherent culture was used to obtain EMSCs[7,8]. Briefly, the nasal mucosa lining the respiratory region of the nasal cavity, including the nasal septum and inferior turbinate, was carefully isolated and completely cut into pieces. The pieces of respiratory mucosa tissue were cultured in DMEM/F12 containing 10% FBS, 2 mM L-glutamine, and 100 U/mL penicillin–streptomycin in plastic flasks at 37 °C in 5% CO_2. After ~14 days, the cells had migrated from the tissue. The cells were passaged upon reaching 90% confluence, and cells from the seventh passage were used in all of our assays. To detect the expression of stem cell markers, passaged EMSCs were cultured on poly-L-lysine-coated glass coverslips and fixed using 4% paraformaldehyde at 90% confluence. The cells were subjected to immunofluorescence staining with antibodies against various stem cell markers, including vimentin, nestin, and S100. Briefly, the cells were fixed with 4% paraformaldehyde at 4 °C for 12 h, washed with phosphate-buffered saline (PBS), and treated with 0.3% Triton X-100/2% bovine serum albumin. Finally, the cells were incubated with primary antibodies overnight at 4 °C. After washing three times, the cells were incubated with secondary antibodies for 2 h at 37 °C. The nuclei were visualized by counterstaining with DAPI (4′,6-diamidino-2-phenylindole). The stained cells were observed under an immunofluorescence microscope (Axio Observer, ZEISS, Germany).

Construction of TG2-GFP gene recombinant adenoviruses and transduction into EMSCs

The following primers were designed for PCR to synthesize the rat TG2 (rTG2) gene (2061 bp): TG2-f, CTAGCTAGCGCCACCatggccgaggagctgaacct; rTG2-r, GGAATTCttaggccgggccgatgatga. A recombinant rTG2 adenovirus shuttle plasmid was constructed by Nanjing GenScript Bioengineering Technology and Services Co., Ltd (Nanjing, China) and was confirmed by sequencing. Briefly, TG2 genes were inserted into a pAdShuttle-IRES-hrGFP2-TG2 vector to prepare the shuttle vector, and the pAdShuttle-IRES-hrGFP2 vector was set as a parallel

group. The 293A cells were provided by the Shanghai Institute of Biochemistry and Cell Biology (Shanghai, China). The 293A cells ($2 × 10^6$ cells/well) were seeded in 6-cm^2 dishes in DMEM supplemented with 10% FBS and incubated at 37 °C in 5% CO_2 overnight. The medium was replaced before transfection. The cells were transfected at 80–90% confluence with pacAd5-9.2-100 and the pAdShuttle-IRES-hrGFP2-TG2 shuttle plasmid using Lipofectamine 2000 (Invitrogen, CA, USA) according to the manufacturer's instructions. Twelve days after transfection, recombinant adenoviruses harboring the TG2 (Ad-TG2-GFP) gene were harvested. All recombinant adenoviruses were amplified in 293A cells (ATCC, CA, USA) and purified using double cesium chloride density gradient ultracentrifugation. Titers of the adenoviral stocks were determined using a plaque assay in 293A cells. EMSCs ($2 × 10^5$) at passage 7 were infected with Ad-TG2-GFP or Ad-GFP adenoviruses following standard infection procedures. TG2-GFP-EMSCs (TG2-EMSCs) and GFP-EMSCs (GFP-EMSCs) were harvested, and TG2-GFP and GFP gene expression levels were detected under a fluorescence microscope. The TG2 protein expression in the TG2-EMSCs was determined by immunofluorescence staining. The expression of stem cell markers, including vimentin, nestin, and S100, in the TG2-EMSCs was detected by immunofluorescence staining. The levels of extracellular and intracellular TG2 protein expression were determined by Western blotting (see Supplementary information for experimental details).

Preparation of the fibrin scaffold and assay of the growth characteristics of the EMSCs and TG2-EMSCs in the scaffold

The fibrin scaffold was prepared according to the method described in our previous study[8]. Briefly, the fibrin scaffold was formed by mixing two separate solutions at a 1:1 (vol/vol) ratio to obtain a final fibrinogen concentration of 50 mg/ml: solution A consisted of 100 mg/ml rat fibrinogen dissolved in PBS, and solution B contained 100 U of rat thrombin dissolved in 5 ml of PBS. The fibrinogen/thrombin mixture was immediately and evenly dropped onto 96-, 48-, or 6-well cell culture plates, and the plates were incubated at 37 °C for 30 min. For cell seeding, EMSCs and TG2-EMSCs were digested with trypsin and then transferred to the 48-well (approximately $2 × 10^4$ cells) or 6-well (approximately $5 × 10^5$) plates, and an adequate amount of fresh medium was added. The structure of the fibrin scaffold was examined by scanning electron microscopy (SEM, JSM-6000, Japan) and transmission electron microscopy (Philips-Tecnai12, The Netherlands). The growth pattern of the EMSCs seeded on the fibrin scaffold for 7 days was also observed by SEM. Furthermore, the expression of BMP-2, VEGF, LN, and FN in TG2-EMSCs was detected via immunofluorescence staining. The differences in the expression of proteins,

including VEGF, BMP-2, TG2, FN, and LN, among the TG2-EMSCs, GFP-EMSCs, and EMSCs in the fibrin scaffold, were analyzed by Western blotting.

To determine whether the overexpression of TG2 influenced the proliferation of EMSCs, an MTT (3-(4,5-dimethylthiazol-2-yl)-2,5-diphenyltetrazolium bromide) assay was performed. More details can be found in the Supplementary information.

Fibrin scaffold calcification in vitro

In this study, a fibrin scaffold was used as the substrate for the proliferation and osteogenic differentiation of EMSCs. The calcification of the fibrin scaffold in vitro was examined to further verify whether the fibrin scaffold was an ideal functional biomaterial for bone tissue engineering.

ALP-induced calcification of the cell-free fibrin scaffold in vitro

The cell-free fibrin scaffold was immersed in osteogenic induction medium containing ALP for 14 days to evaluate the function of this scaffold as the ideal substrate for calcium deposition in an osteogenic microenvironment. Briefly, the fibrin scaffold without cells was prepared as previously described and then calcified by immersion in osteogenic medium (15% FBS, 0.1 nM dexamethasone, 10 mM β-glycerophosphate, 0.01 μM 1,25-dihydroxy vitamin D3, and 50 μM ascorbic acid in α-MEM) containing exogenous ALP (100 U/ml) for 14 days. During the induction process, half of the medium containing exogenous ALP was changed every 2 days. After induction, calcium nodule formation was assessed by alizarin red S staining. Meanwhile, the cell-free fibrin scaffold immersed in osteogenic medium without ALP for 14 days was used as the control.

Osteogenic differentiation of EMSCs and TG2-EMSCs seeded on the fibrin scaffold

To investigate the promoting effect of TG2 on the osteogenic differentiation of EMSCs in the fibrin scaffold, EMSCs and TG2-EMSCs were seeded on 48- or 6-well plates coated with the fibrin scaffold. Then, osteogenic differentiation was induced using osteogenic medium (without additional ALP) for 14 days. After inducing differentiation, the expression of BMP-2, VEGF, COL I, OCN, and OPN in the EMSCs, GFP-EMSCs, and TG2-EMSCs was detected via immunofluorescence staining. Differences in the expression of these proteins, including VEGF, BMP-2, OPN, OCN, and COL I, among the TG2-EMSCs, GFP-EMSCs, and EMSCs in the fibrin scaffold, were analyzed by Western blotting.

In addition, to explore the role of TG2 in the osteogenic differentiation of EMSCs, an inhibition experiment was performed as follows: TG2-EMSCs were seeded in 48- or 6-well plates with osteogenic medium and allowed to adhere for 24 h. Then, TG2-EMSCs were treated with 0.5 mM CYS to inhibit TG2 activity[27]. After 14 days of inducing differentiation, mineralized nodules were stained with alizarin red S, and the ALP activity of the cells was evaluated using NBT/BCIP (nitro blue tetrazolium/5-bromo-4-chloro-3-indolyl phosphate) staining. All images were captured under a Zeiss microscope (Axio Observer, ZEISS, Germany). ImageJ software was used to quantify the stained areas. Differences in the expression of these proteins, including VEGF, BMP-2, OPN, OCN, and COL I, among the TG2-EMSCs, TG2-EMSCs + CYS, and EMSCs in the fibrin scaffold, were analyzed by Western blotting. Moreover, to investigate which part of TG2 could promote EMSC osteogenic differentiation, we conducted three additional experiments, which are described in the Supplementary information.

Preparation and morphological observation of the bone-like graft made of TG2-EMSCs and the fibrin scaffold

To prepare tissue-engineered bone-like grafts made of TG2 gene-modified EMSCs and the fibrin scaffold for transplantation, TG2-EMSCs seeded on the fibrin scaffold were cultured in osteogenic medium for 21 days, leading to sufficient calcification of the scaffold. The surface structure of the calcified fibrin scaffold (bone-like graft) was observed with a phase-contrast microscope. Meanwhile, the OCN expression of the osteoblasts/osteocytes in the mineralized scaffold was evaluated by immunofluorescence staining, and calcification was assessed by alizarin red S staining.

Efficient extraction of proteins from the fibrin scaffold with seed cells and detection of the expression levels of proteins of interest by Western blotting

To analyze differences in the expression of proteins of interest among the groups, including the TG2-EMSC/fibrin, TG2-EMSC + CYS/fibrin, and EMSC/fibrin groups, fibrin scaffolds with seed cells were dissolved by nattokinase for protein extraction due to the specific and high fibrinolytic activity of nattokinase[28]. Briefly, a fibrinolytic solution was prepared by dissolving 50 FU/mL nattokinase in PBS containing 1 mM EDTA. Fibrin scaffolds containing cells were washed with PBS and subsequently dissolved by the addition of 250 μl of the nattokinase solution and incubation at 37 °C. The incubation times were determined empirically. The dissolved samples were ultrasonicated at 4 °C, and then the homogenates were mixed with equal volumes of RIPA buffer containing a protease inhibitor cocktail and EDTA. The above lysates were centrifuged at $12,000 \times g$ for 5 min. The protein concentrations of the supernatant were determined using a BCA kit (Thermo Fisher Scientific, Rockford, IL, USA). Finally, the expression levels of the proteins of interest, including TG2, BMP-2, VEGF, COL I,

LN, FN, OCN, and OPN, were detected by Western blotting as follows: The supernatant containing the proteins of interest was mixed with equal amounts of loading buffer and then heat denatured at 100 °C for 5 min. An equal amount of protein from each sample was loaded into 8% polyacrylamide gels, separated by sodium dodecyl sulfate-polyacrylamide gel electrophoresis, and transferred to a polyvinylidene difluoride (PVDF) membrane (Millipore, Temecula, CA, USA) by electrophoresis. The PVDF membrane was incubated with antibodies against the proteins of interest and β-tubulin (as a standard control), followed by incubation with horseradish peroxidase-conjugated secondary antibodies (Santa Cruz). The protein bands were visualized using a Pierce ECL Plus substrate (Thermo Fisher Scientific) and scanned with a Typhoon 9400 Variable Mode Imager (Amersham Biosciences, UK). β-Tubulin served as the internal reference. Each experiment was repeated at least three times for statistical analysis.

Transplantation of the TG2-EMSC/fibrin scaffold for bone defect repair and evaluation of the therapeutic efficacy

In this study, all animal experimental protocols were approved by the Jiangsu University Ethics Committee for the use of experimental animals and conformed to the Guide for the Care and Use of Laboratory Animals. The surgical procedures were as follows: SD rats (200 g) were anesthetized, and then an 8-mm-diameter calvarial critical-sized defect was created in the calvarial bone using a dental bur attached to a low-speed handpiece with minimal invasion of the dura mater. The rats were divided into the following three groups, with 10 animals per group: group 1, transplanted fibrin scaffolds without cells; group 2, transplanted EMSC-loaded fibrin scaffolds; and group 3, transplanted TG2-EMSC-loaded fibrin scaffolds (tissue-engineered bone-like grafts). The EMSC-loaded fibrin scaffolds and TG2-EMSC-loaded fibrin scaffolds were constructed according to the following procedure. The cells were seeded on 6-well plates coated with fibrin gel in normal medium. After 24 h, these cells were cultured in osteogenic induction medium. After 21 days of osteogenic differentiation induction, the partially calcified fibrin scaffold was overturned, and fresh EMSCs or TG2-EMSCs were reseeded on the other surface of the scaffold. Twenty-four hours later, the fibrin scaffolds loaded with differentiated (21 days of induction) and undifferentiated cells (newly seeded) were shaped into a circular pattern with a diameter of 8 mm and then transplanted into the critical-sized calvarial defect area. Then, the gap between the fibrin scaffold and the normal bone around the defect was filled with fresh fibrin gel, encapsulating the EMSCs or TG2-EMSCs. After 4 weeks, five rats from each group were sacrificed by deep anesthetization with an intraperitoneal injection of phenobarbital sodium (200 mg/kg), and skull specimens were fixed in 4% paraformaldehyde overnight at 4 °C. Then, the specimens were decalcified in 10% EDTA in phosphate buffer (pH 7.4) for 7 days at 4 °C. After dehydration in a graded series of ethanol solutions, the tissue was embedded in paraffin. Serial longitudinal tissue sections were prepared and subjected to staining and observation, as follows. Skull specimens were cut into 5 μm sections, which were stained with hematoxylin and eosin (H&E) for evaluation of the reparative effect. The expression of TG2 and OCN in the new bone over the defect area was detected by immunohistochemistry. To evaluate the therapeutic efficacy of these grafts in defect repair, the thickness of the regenerative tissue (at the center point) in the defect area in the EMSC/fibrin group and the TG2-EMSC/fibrin group was measured, and then the average thickness for each animal (five sections from one animal for five animals) was calculated and compared by statistical analyses to show the difference between the EMSC/fibrin group and the TG2-EMSC/fibrin group ($n = 5$).

Examination of the skull by CT and gross observation

The remaining 15 experimental rats (five rats per group) were examined by computed tomography (CT) at 1, 4, 8, and 12 weeks postimplantation. Imaging of the skull was performed using a Gamma Medica X-SPECT small-animal system (Gamma Medica, Salem, NH) with a peak voltage of 120 kV and current of 150 mA. Three-dimensional reconstruction software was used for quantitative analysis of the therapeutic efficacy of the transplanted grafts in bone defect repair. The bone volume (BV, mm^3) and the tissue volume (TV, mm^3) were measured. The percent BV (BV/TV, %) was calculated and compared by statistical analyses to show differences in bone defect healing among the TG2-EMSC/fibrin, EMSC/fibrin, and fibrin groups ($n = 5$).

Gross examination of the skull was performed following animal sacrifice after CT analysis. The experimental animals were sacrificed at 12 weeks after transplantation of the different grafts, and the gross appearance of the skull was observed.

Statistical analyses

All values are reported as the mean ± standard deviation (SD). One-way ANOVA with a Tukey's multiple comparison post hoc test was performed to determine statistically significant differences among conditions. $*P < 0.05$ and $**P < 0.01$ were considered statistically significant.

Results

Schematic illustration of the procedure for preparing the functional tissue-engineered bone-like graft

Figure 1A shows a diagram of the tissue-engineered bone-like graft, and Fig. 1B presents a schematic of the transplantation procedure.

Fig. 1 Preparation of functional tissue-engineered bone-like grafts. A Step-by-step procedures for preparing functional tissue-engineered bone-like grafts. **B** Schematic drawing of transplantation procedure.
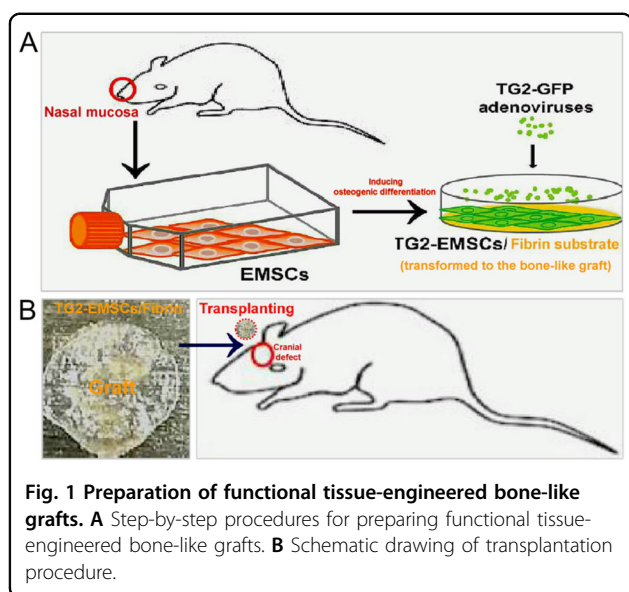
Morphology and stemness of EMSCs isolated from the nasal mucosa before and after modification with the TG2 gene

The adherent EMSCs from the lamina propria of the nasal mucosa migrated and expanded easily in vitro, and the cultured cells progressively exhibited a fibroblast-like morphology (Fig. 2A). Immunofluorescence staining revealed that most EMSCs expressed neural crest cell and mesenchymal stem cell markers, including vimentin, nestin, and S100 (Fig. 2B). Moreover, green fluorescence from GFP in EMSCs was detected at 48 h after TG2-GFP adenovirus transfection. Moreover, TG2 overexpression was detected by immunofluorescence staining, indicating the high efficiency of gene transfection (Fig. 2C). To determine the phenotypical profiles of the TG2-EMSCs, immunofluorescence staining was performed to assess the expression of stem cell markers, including vimentin, nestin, and S100. The results show that the TG2-EMSCs expressed both TG2 (Fig. 2C) and stem cell markers (Fig. 2D). The expression levels of intracellular and extracellular TG2 in TG2-EMSCs were significantly higher than those in GFP-EMSCs and EMSCs. Representative images of the levels of intracellular and extracellular TG2 expression in TG2-EMSCs are shown in the Supplementary information (Supplementary Figs. 1 and 2).

Biological characteristics of EMSCs and TG2-EMSCs seeded in the fibrin scaffold

The fibrin scaffolds showed a semitransparent gel-like appearance (Fig. 3A1). These scaffolds possessed a sponge-like structure, as observed by TEM Fig. 3A2) and SEM (Fig. 3A3). The EMSCs mainly grew on the surface of the fibrin scaffold (Fig. 3A4) due to the presence of fewer ECM proteins cross-linked to the fibrin gel. The
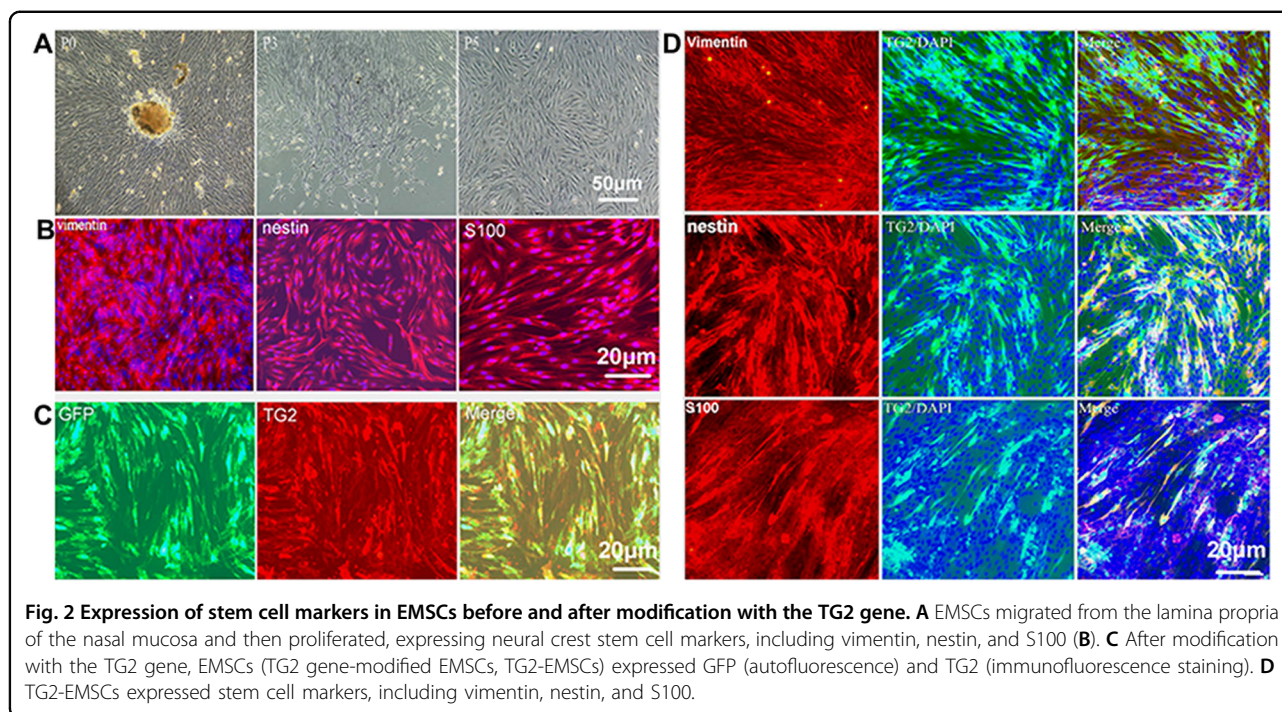
TG2-EMSCs grown on the fibrin gel migrated into the fibrin gel (Fig. 3A5), forming 3D tissue composed of the seed cells and scaffold, because these cells could produce abundant ECM proteins and TG2, which cross-linked more ECM proteins to the fibrin gel. EMSCs (Fig. 3B) and TG2-EMSCs (Fig. 3C) grown on fibrin scaffolds expressed ECM proteins and cell growth factors, including BMP-2, VEGF, LN, and FN. The expression levels of these proteins and TG2 were detected by Western blotting, which showed bands for more proteins of interest with different molecular weights in the TG2-EMSC group, suggesting cross-linking by TG2 (Fig. 3D). Quantitative analysis of the relative content of these proteins (Fig. 3E) indicated that the content of these proteins was significantly higher in the TG2-EMSC/fibrin scaffold than in the controls (GFP-EMSC/fibrin scaffold and EMSC/fibrin scaffold). Each bar represents the mean value ± SD of measurements made in three independent replicates. Moreover, the MTT results demonstrate that cell proliferation was enhanced by TG2 overexpression (Supplementary Fig. 3).

Differentiation of TG2-EMSCs into osteoblasts in the fibrin scaffold

After 14 days of culture in osteogenic medium, TG2-EMSCs transformed into osteoblast-like cells, which more strongly expressed bone matrix proteins (Fig. 4A), including OPN, OCN, and COL I, and growth factors (Fig. 4B), including BMP-2 and VEGF, than the control cells. The results of immunofluorescence staining for OCN, OPN, COL I, BMP-2, and VEGF in GFP-EMSCs are shown in Supplementary Fig. 4. The OCN, OPN, COL I, BMP-2, and VEGF protein levels were determined by Western blotting (Fig. 4C). As shown in Fig. 4D, the expression levels of these proteins, including VEGF, BMP-2, OPN, OCN, and COL I, in TG2-EMSCs were significantly higher than those in EMSCs. However, there were no significant differences in protein expression between the GFP-EMSC and the EMSC groups. In addition, bands of more proteins of interest with different molecular weights were observed in the TG2-EMSC group, suggesting cross-linking of the proteins by TG2.

Mineralization of and ALP activity in the TG2-EMSC/fibrin scaffold

To detect calcification of the fibrin scaffold, alizarin red S staining was performed to observe mineralized nodule formation in the scaffold after 14 days of osteogenic differentiation induction. The results showed many mineralized nodules in the TG2-EMSC/fibrin scaffold (Fig. 5A1). Meanwhile, the TG2-EMSCs seeded in the fibrin scaffold exhibited strong ALP activity (Fig. 5B1). To verify the function of TG2 in osteogenic differentiation, CYS was employed to inhibit TG2 activity during the induced differentiation of TG2-EMSCs in the fibrin scaffold.

Fig. 2 Expression of stem cell markers in EMSCs before and after modification with the TG2 gene. A EMSCs migrated from the lamina propria of the nasal mucosa and then proliferated, expressing neural crest stem cell markers, including vimentin, nestin, and S100 (**B**). **C** After modification with the TG2 gene, EMSCs (TG2 gene-modified EMSCs, TG2-EMSCs) expressed GFP (autofluorescence) and TG2 (immunofluorescence staining). **D** TG2-EMSCs expressed stem cell markers, including vimentin, nestin, and S100.

Mineralization and ALP activity were significantly inhibited by treatment with CYS (Fig. 5A2, B2). Alizarin red S (Fig. 5A3) and ALP (Fig. 5B3) staining indicated the presence of mineralized nodules and ALP activity in EMSCs after osteogenic induction. Quantitative analysis indicated that the degree of mineralization and ALP activity was highest in the TG2-EMSC/fibrin groups among the TG2-EMSC/fibrin, TG2-EMSC + CYS/fibrin, and EMSC/fibrin groups (Fig. 5C, D). Furthermore, after treatment with the inhibitor, the OCN, COL I, OPN, VEFG, and BMP-2 expression levels were dramatically decreased (Fig. 5E, F). These results suggest that TG2 played an important role in the osteogenic differentiation of TG2-EMSCs in the fibrin scaffold. Moreover, our findings indicate that extracellular TG2 played a major role in promoting the osteogenic differentiation of EMSCs (Supplementary Figs. 5–10). More details of the study design are described in the Supplementary information.

Histological characteristics of the calcified cell-free fibrin scaffold and the bone-like graft made of TG2-EMSCs and the fibrin scaffold
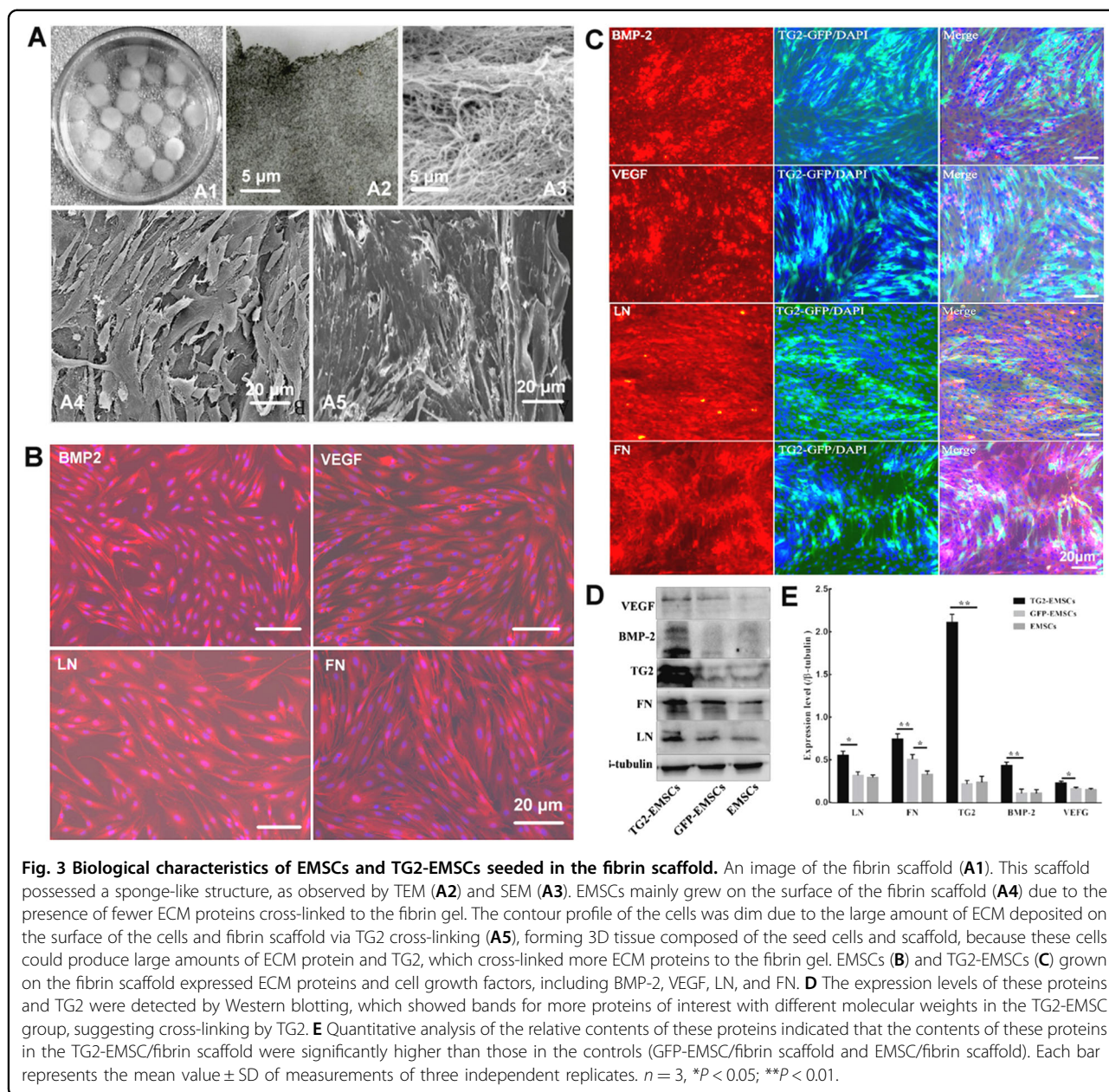
The calcification experiment of the cell-free fibrin scaffold in vitro indicated that the cell-free fibrin scaffold could calcify in osteogenic induction medium containing exogenous ALP. Dense gravel-like mineralized nodules were deposited and uniformly distributed in the fibrin scaffold (Fig. 6A). However, few mineralized nodules were observed in the control group without exogenous ALP (Fig. 6B). These results suggest that the fibrin scaffold was

an ideal substrate for calcium deposition in the osteogenic microenvironment and that calcium deposition onto the scaffold was dependent on the activity of ALP, which could be provided by the seed cells (EMSCs) and/or the intrinsic osteoblasts around the transplantation area in vivo.

As shown in Fig. 6C–F, alizarin red S staining, immunofluorescence, and phase-contrast microscopy indicated that after inducing osteogenic differentiation for 21 days, the TG2-EMSC/fibrin scaffold was transformed into bone-like tissue due to deposition and cross-linking of the bone matrix (osteoid) onto and with the fibrin gel and calcification of the sponge-like scaffold. There were many OCN-positive osteoblasts in the bone-like tissue on immunofluorescence staining. Phase-contrast microscopy showed that the bone-like grafts possessed a rough surface (Fig. 6G). The image in Fig. 6H shows calcification of the fibrin scaffold by alizarin red S staining. This bone-like TG2-EMSC/fibrin graft might support the expected functions of osteogenesis, osteoinduction, and osteoconduction in vivo after transplantation.

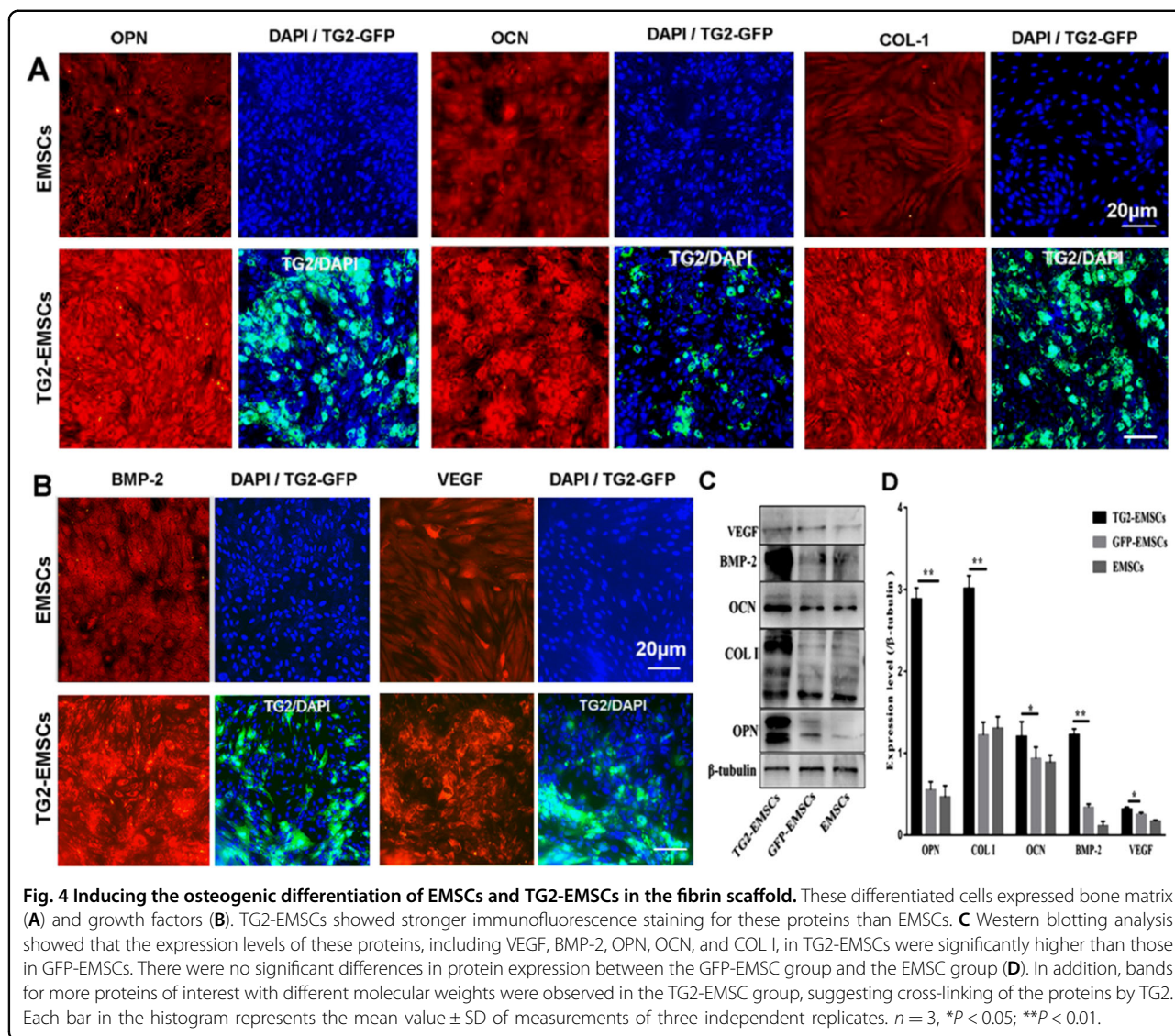### Therapeutic efficacy of the TG2-EMSC/fibrin scaffold (bone-like graft) in calvarial defect repair in rats
Efficiency of intramembranous ossification in the defect area after graft transplantation

The surgical procedure for implanting the TG2-EMSC/fibrin graft is shown in Fig. 7A–C. The fibrin scaffold was cut into a graft 8 mm in diameter (Fig. 7A) and was then transplanted into a critical-sized calvarial defect (Fig. 7B),

Fig. 3 Biological characteristics of EMSCs and TG2-EMSCs seeded in the fibrin scaffold. An image of the fibrin scaffold (**A1**). This scaffold possessed a sponge-like structure, as observed by TEM (**A2**) and SEM (**A3**). EMSCs mainly grew on the surface of the fibrin scaffold (**A4**) due to the presence of fewer ECM proteins cross-linked to the fibrin gel. The contour profile of the cells was dim due to the large amount of ECM deposited on the surface of the cells and fibrin scaffold via TG2 cross-linking (**A5**), forming 3D tissue composed of the seed cells and scaffold, because these cells could produce large amounts of ECM protein and TG2, which cross-linked more ECM proteins to the fibrin gel. EMSCs (**B**) and TG2-EMSCs (**C**) grown on the fibrin scaffold expressed ECM proteins and cell growth factors, including BMP-2, VEGF, LN, and FN. **D** The expression levels of these proteins and TG2 were detected by Western blotting, which showed bands for more proteins of interest with different molecular weights in the TG2-EMSC group, suggesting cross-linking by TG2. **E** Quantitative analysis of the relative contents of these proteins indicated that the contents of these proteins in the TG2-EMSC/fibrin scaffold were significantly higher than those in the controls (GFP-EMSC/fibrin scaffold and EMSC/fibrin scaffold). Each bar represents the mean value ± SD of measurements of three independent replicates. $n = 3$, *$P < 0.05$; **$P < 0.01$.

which could be completely filled with the TG2-EMSC/fibrin graft (Fig. 7C). At 4 weeks after transplantation of the fibrin scaffold without cells, EMSC/fibrin scaffold or TG2-EMSC/fibrin scaffold, coronal tissue sections (stained with H&E) of the skull defect area were observed. The results indicated that there was no regenerative tissue over the defect area in the fibrin scaffold group (Fig. 7D). However, in the EMSC/fibrin scaffold group (Fig. 7E) and the TG2-EMSC/fibrin scaffold group (Fig. 7F), the defect was repaired by a membrane bridge or a bone bridge, respectively. Compared with that in the EMSC/fibrin scaffold group, the bone bridge tissue in the TG2-EMSC/fibrin scaffold group (Fig. 7F) was obviously thicker and

more compact and contained more seed cells (blue nuclei were) and more obvious regenerative bone trabeculae. The image in Fig. 7G is an enlargement of the area in the marked box in Fig. 7F, which shows the characteristics of intramembranous ossification in the graft (TG2-EMSC/fibrin scaffold). The asterisks indicate the bone trabeculae, and the arrowheads indicate the periosteum. The statistical analyses indicated that the average thickness of the regenerative tissue (bone bridge) in the defect area in the TG2-EMSC/fibrin scaffold group (359 ± 35 μm) was significantly thicker than that (117 ± 15 μm) in the EMSC/fibrin scaffold group ($p < 0.01$). These results indicate that transplantation of the TG2-EMSC/fibrin scaffold (bone-

Fig. 4 Inducing the osteogenic differentiation of EMSCs and TG2-EMSCs in the fibrin scaffold. These differentiated cells expressed bone matrix (**A**) and growth factors (**B**). TG2-EMSCs showed stronger immunofluorescence staining for these proteins than EMSCs. **C** Western blotting analysis showed that the expression levels of these proteins, including VEGF, BMP-2, OPN, OCN, and COL I, in TG2-EMSCs were significantly higher than those in GFP-EMSCs. There were no significant differences in protein expression between the GFP-EMSC group and the EMSC group (**D**). In addition, bands for more proteins of interest with different molecular weights were observed in the TG2-EMSC group, suggesting cross-linking of the proteins by TG2. Each bar in the histogram represents the mean value ± SD of measurements of three independent replicates. $n = 3$, *$P < 0.05$; **$P < 0.01$.

like graft) could promote intramembranous ossification of the graft for defect repair.

Osteogenic differentiation of TG2-EMSCs and vascularization of the bone-like graft in vivo

To confirm the in vivo osteogenic differentiation of the TG2-EMSCs in the regenerative bone bridge (Fig. 8A), immunohistochemical staining for TG2 and OCN in adjacent tissue sections (with similar structures and seed cells) was performed to detect osteoblasts/osteocytes derived from the TG2-EMSCs in the regenerative tissue. As shown in Fig. 8B, TG2-positive cells were observed in the regenerative tissue in the defect area. Moreover, these cells also expressed OCN (Fig. 8C). This finding suggests that TG2-EMSCs could maintain the differentiated phenotype of osteoblasts/osteocytes and produce bone matrix in the graft in vivo (Fig. 8D). Moreover, around these cells,

there were densely distributed regenerative blood vessels (asterisks in Fig. 8D) in the graft, suggesting that the TG2-EMSC/fibrin scaffold (bone-like graft) could be vascularized in vivo.

CT analysis

New bone formation in the bone defect was dynamically evaluated using quantitative CT after implantation of the three kinds of grafts. The 3D reconstructions (Fig. 9A) indicated obvious new bone formation in the bone defect at 4, 8, and 12 weeks in the TG2-EMSC/fibrin group. However, the EMSC/fibrin group showed little bone formation, and the control group (fibrin group) showed poor bone healing at all time points. Quantitative analysis of the CT data in Fig. 9B indicated that the ratio of the regenerated BV to the total (defect) volume (BV/TV) in the TG2-EMSC/fibrin group was significantly higher than

Fig. 5 Mineralization of and alkaline phosphatase activity in the TG2-EMSC/fibrin scaffold. Alizarin red S staining was performed to observe mineralized bone nodules in scaffolds loaded with TG2-EMSCs (**A1**), TG2-EMSCs+CYS (**A2**), and EMSCs (**A3**). Many mineralized nodules were observed in the TG2-EMSC/fibrin scaffold; however, CYS inhibited mineralization. Meanwhile, the TG2-EMSC/fibrin scaffold groups exhibited stronger ALP activity (**B1**) than the other groups (**B2**, **B3**). Quantitative analysis of the results shown in (**C**, **D**), $n = 3$, $**P < 0.01$. **E** Western blotting results showing the expression levels of VEGF, BMP-2, OPN, OCN, and COL I in the three groups. **F** Quantification analysis indicated that the content of proteins of interest was highest in the TG2-EMSC/fibrin group. $n = 3$, $**P < 0.01$.

that in the EMSC/fibrin group, while the BV/TV in the EMSC/fibrin group was significantly higher than that in the control group (fibrin group). The BV/TV in the control group (fibrin group) was the lowest among the three groups at all time points. Altogether, these data indicate that the novel functional tissue-engineered bone-like grafts made of TG2 gene-modified EMSCs and fibrin scaffolds substantially improved bone regeneration.

Gross appearance of the cranial bone at 12 weeks after graft transplantation into the defect

In the TG2-EMSC/fibrin group (Fig. 10A), the cranial defect was almost fully repaired by the regenerative bone. In the EMSC/fibrin group (Fig. 10B), the cranial defect was partially repaired, and the translucent area of the defect was observed due to the smaller amount and thinner layer of regenerative bone, but the repaired area of the defect was larger in the EMSC/fibrin group than in the fibrin group. In the fibrin group (Fig. 10C), almost no cranial defect repair was present, and a large translucent area of the defect was observed. Interestingly, in the EMSC/fibrin group and the fibrin group, there were many regenerative blood vessels radially distributed in the regenerative tissue of the defect area, especially in the fibrin group, and the blood vessels were more densely distributed. These results demonstrate that transplantation of the TG2-EMSC/fibrin scaffold resulted in better bone regeneration than transplantation of the other two grafts and that the transplanted fibrin scaffold could promote neovascularization in the regenerative tissue at
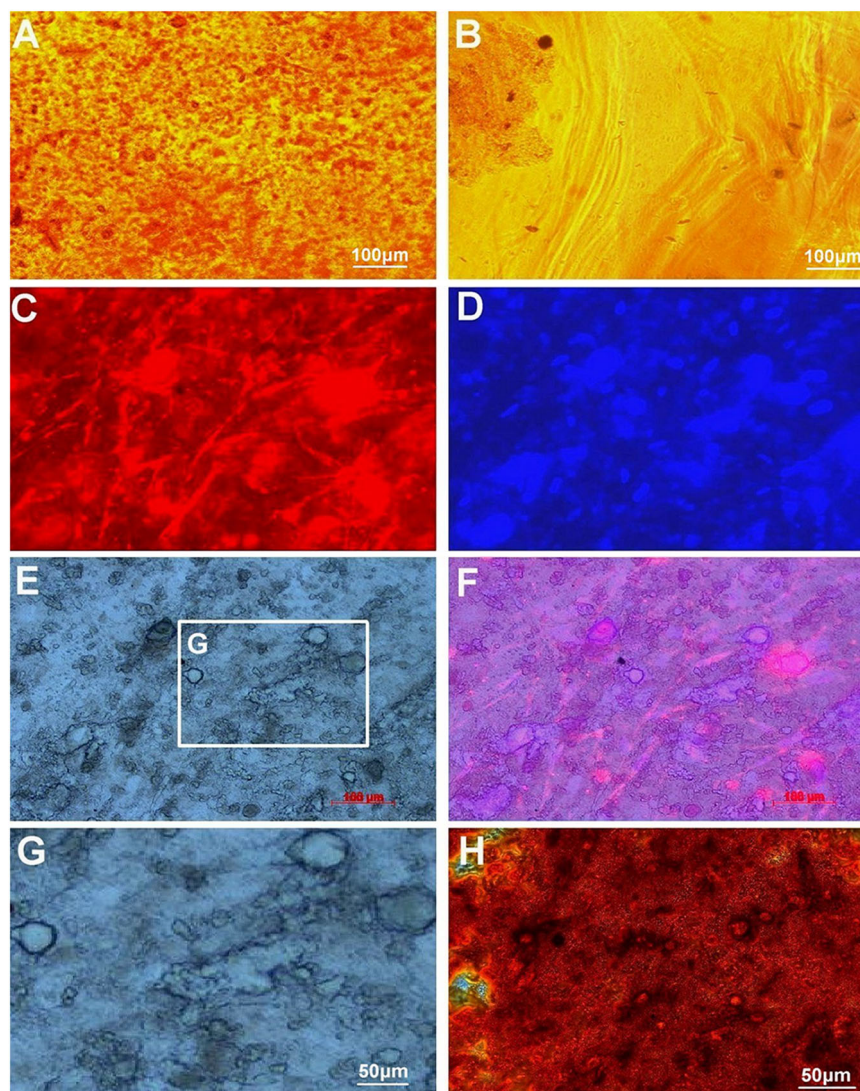
Fig. 6 Histological characteristics of the bone-like graft made of TG2-EMSCs and the fibrin scaffold for transplantation. A Calcification of the fibrin scaffold without cells after induction via an osteogenic medium with ALP by alizarin red S staining. **B** Little calcium deposition is shown by alizarin red S staining in the cell-free fibrin scaffold induced via osteogenic medium without ALP. **C**, **F** TG2-EMSCs seeded in the fibrin scaffold were induced to differentiate into osteoblasts/osteocytes, which were buried in bone-like tissue and expressed OCN (**C**). DAPI staining of the nuclei of the cells in the graft (**D**). Observation by phase-contrast microscopy showed the rough surface of the fibrin scaffold due to calcium deposition (**E**). **F** Merged image of (**C**–**E**). **G** An enlargement of the area in the marked box of (**E**) to show extensive insoluble calcium salt deposition, which formed the rough surface of the graft. **H** Calcification of the TG2-EMSC/fibrin graft by alizarin red S staining.

the site of the cranial defect. Representative images of H&E-stained sections (Supplementary Fig. 11) and coronal micro-CT images (Supplementary Fig.12) of the skull defect area in an experiment animal from each group at 12 weeks are provided in the Supplementary information.

Discussion

Previous studies performed by our group and other researchers have shown that EMSCs represent a type of multipotent adult stem cell derived from cranial neural crest cells[7,8]. These stem cells can differentiate into specific phenotypes, such as osteoblasts, adipocytes, chondrocytes, and neurons, in vitro. Furthermore, the EMSCs seeded on the fibrin scaffold described in our previous study demonstrated the capacity to proliferate extensively and maintain their capacity to differentiate into multiple cell types in vitro. Based on their stemness, EMSCs might be applied as seed cells in scaffold transplantation to repair tissue injuries, such as bone defects. Among tissue engineering strategies for the repair of tissue injuries, in addition to stem cell transplantation, genetic therapy has become a promising
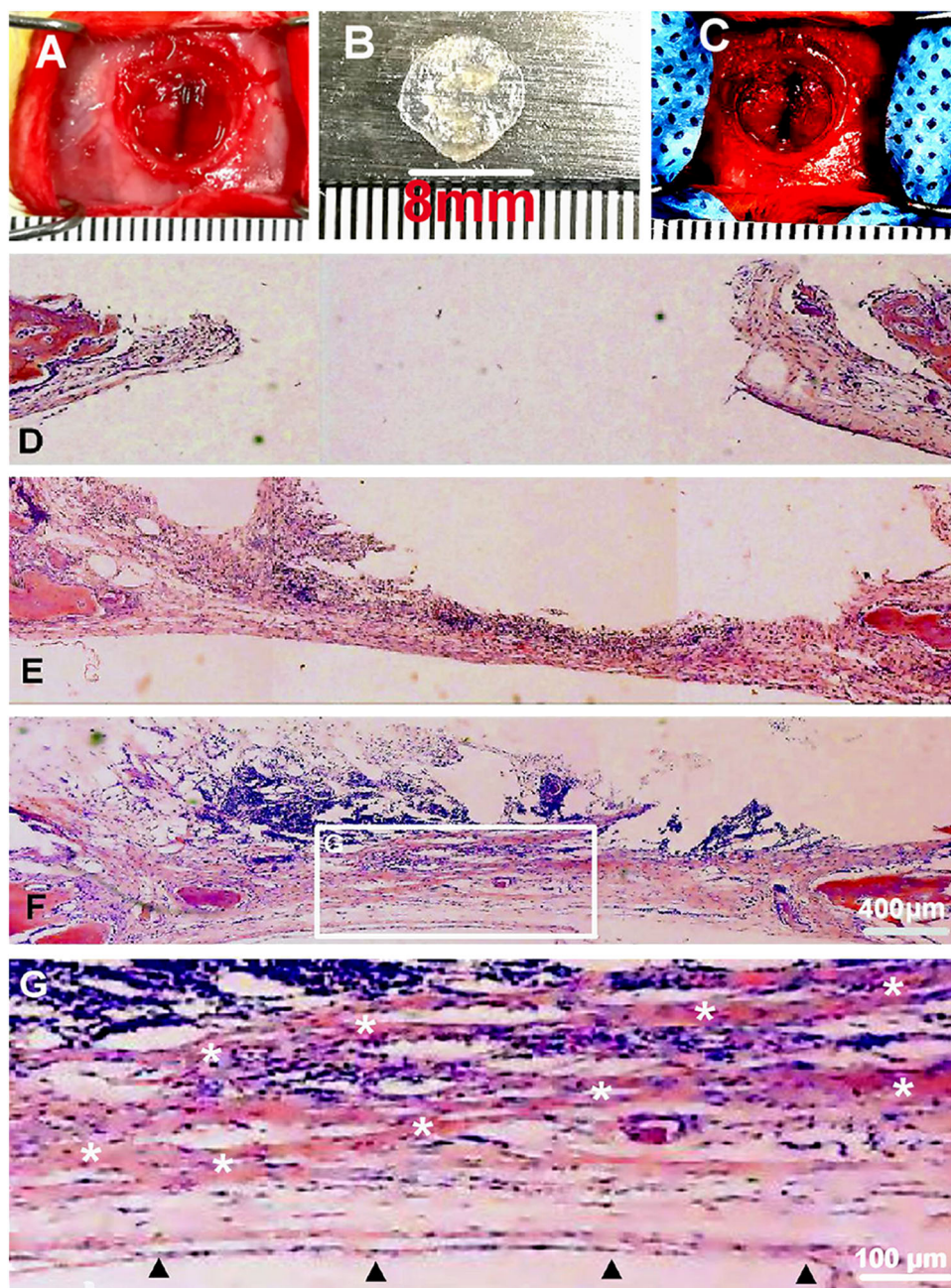
Fig. 7 Surgical procedure for TG2-EMSC/fibrin graft implantation and histological observation of the regenerated tissue bridge covering the calvarial defect. A Calvarial defect 8 mm in diameter. **B** TG2-EMSC/fibrin graft. **C** Implantation of the graft into the calvarial defect. At 4 weeks after transplantation, histological observation of coronal H&E-stained tissue sections of the skull defect indicated no regenerative tissue over the defect in the fibrin group (**D**). However, in the EMSC/fibrin group (**E**) and the TG2-EMSC/fibrin group (**F**), the defect was repaired by a membrane bridge or bone bridge, respectively. The bone bridge tissue in the TG2-EMSC/fibrin group (**F**) was obviously thicker and more compact and contained more seed cells (blue nuclei) and more obvious regenerative bone trabeculae than the corresponding tissue in the EMSC/fibrin group (**E**). **G** An enlargement of the area in the marked box in (**F**), which shows the characteristics of intramembranous ossification in the graft (TG2-EMSC/fibrin scaffold). The asterisks indicate bands of collagen fibers, and the arrowheads indicate the periosteum.

approach, and adenoviruses have become important transgenic vectors for effective clinical gene therapy[29]. Mounting reports have indicated that TG2 plays an important role in stem cell differentiation[30,31]. For example, Yin et al.[32] found that SAOS-2 cells exhibit high levels of TG2 expression and activity during the progression of osteoblast differentiation. Moreover, TG2 could cross-link some soluble growth factors and
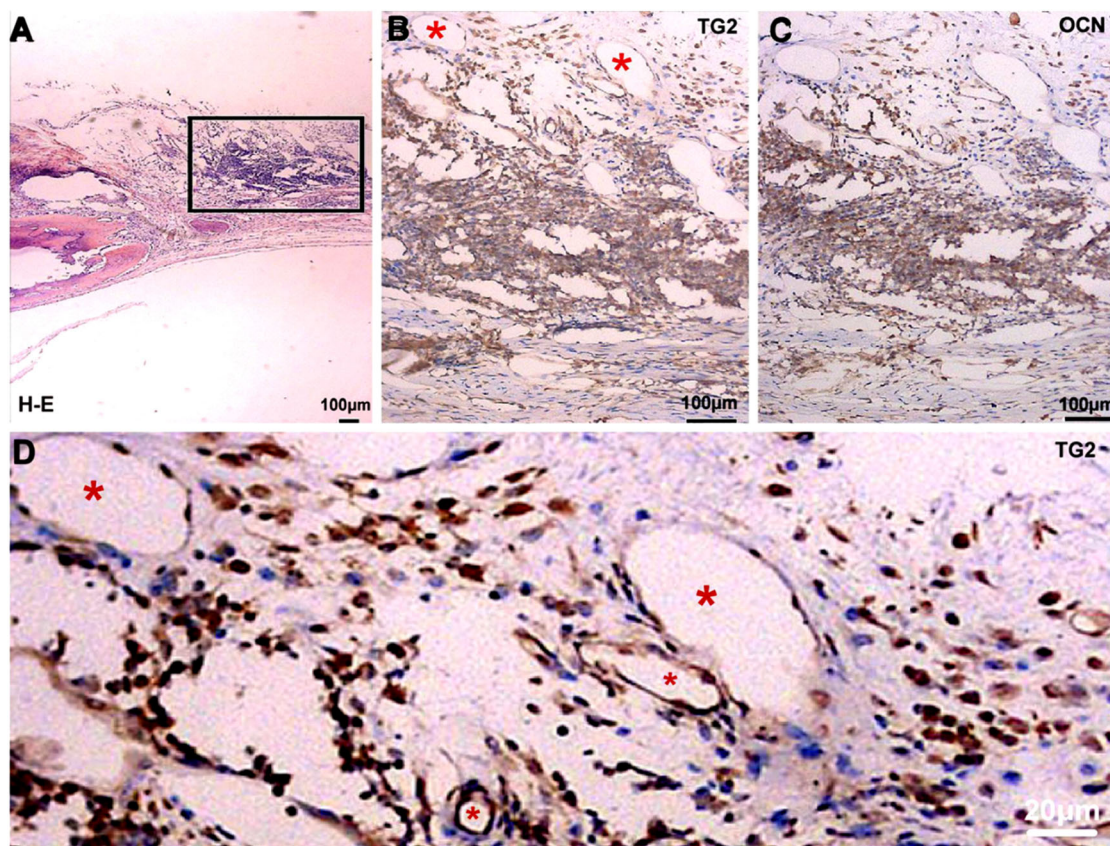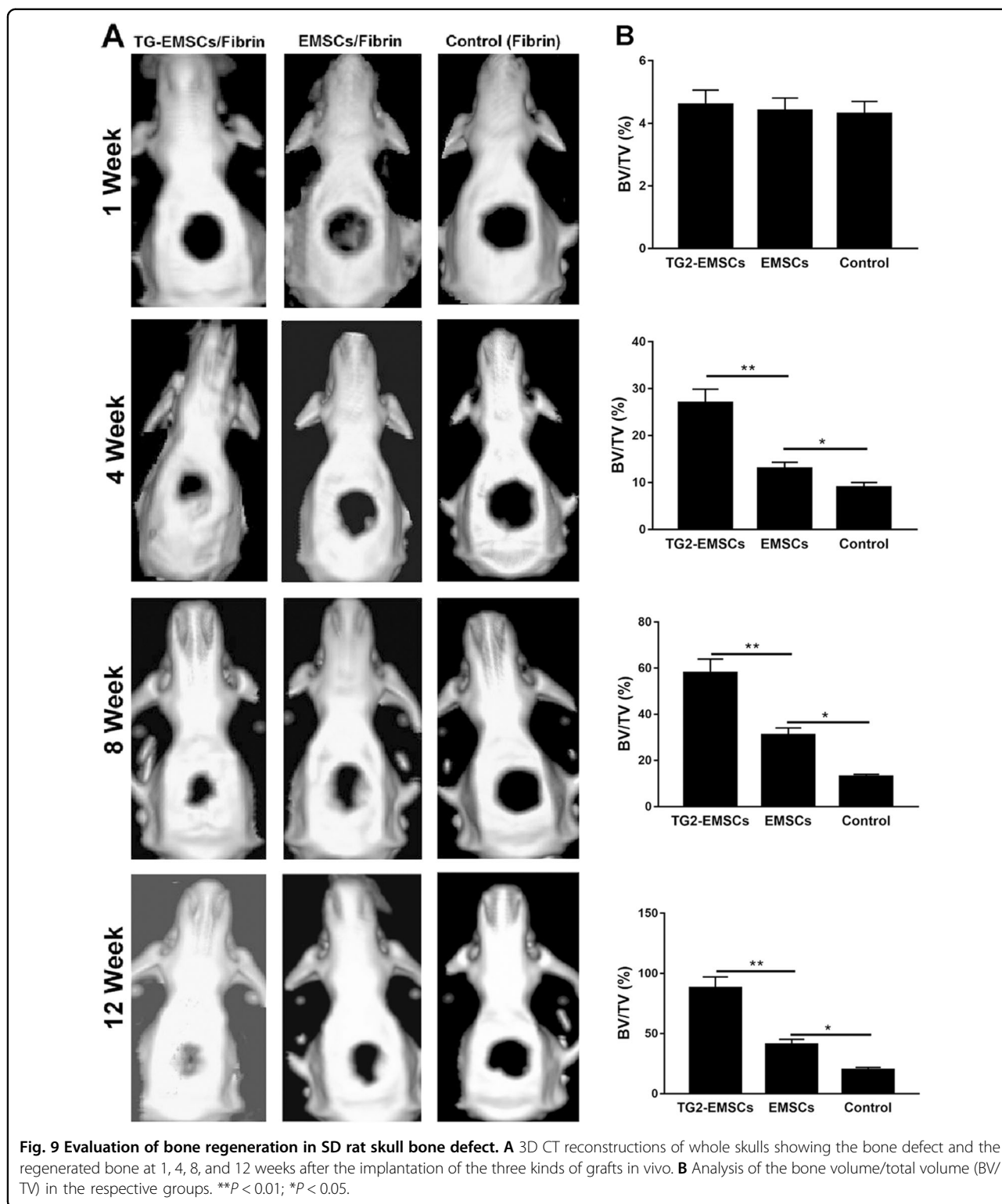
Fig. 8 Observation of the osteogenic differentiation of TG2-EMSCs and regenerative blood vessels in the bone bridge. To confirm the in vivo osteogenic differentiation of the TG2-EMSCs in the transplanted bone-like graft into osteoblasts/osteocytes, cells coexpressing TG2 and OCN were detected by the immunohistochemical staining of adjacent tissue sections among continuous coronal plane sections (**A–C**). At 4 weeks after implantation of the graft, TG2-EMSCs could express both TG2 (**B**) and OCN (**C**) within the regenerative bone bridge (marked box in **A**). Meanwhile, there were densely distributed regenerative blood vessels (asterisks) in the graft. Around the vessels, there were many TG2-positive osteoblasts/osteocyte-like cells observed on immunostaining (**D**), which might be derived from TG2-EMSCs.

ECM proteins and then promote the deposition of these proteins into tissue[17]. Given these interesting findings, the present study first investigated the role of TG2 overexpression in the osteogenic differentiation of EMSCs seeded in a fibrin scaffold and then constructed a novel functional tissue-engineered bone-like graft made of TG2 gene-modified EMSCs and a fibrin scaffold for bone defect repair.

The results demonstrated high levels of both extracellular and intracellular TG2 expression in EMSCs after TG2 gene transfection. Moreover, immunofluorescence staining showed that TG2-EMSCs and EMSCs strongly expressed not only mesenchymal cell and neural crest cell markers, including vimentin, S100, and nestin, but also BMP-2, VEGF, COL I, LN, and FN. The results of Western blotting showed that the BMP-2, VEGF, COL I, LN, FN, and TG2 expression levels in the TG2-EMSCs were significantly higher than those in the controls. Because ECM and growth factors play significant roles in the

process of bone development, these interesting findings strongly suggest that the transplantation of TG2-EMSCs seeded in fibrin scaffolds may provide a new therapeutic approach for bone defect repair.

In the osteogenic differentiation experiments, the results of immunofluorescence staining and Western blotting showed higher expression levels of osteogenic markers, including COL I, OCN, and OPN, in the TG2-EMSCs than in the control cells. In the TG2-EMSC/fibrin scaffold, many mineralized nodules were observed by alizarin red S staining, combined with strong ALP activity, suggesting that TG2-EMSCs possessed greater potential for osteogenic differentiation. Furthermore, the results of the TG2 activity inhibition experiments indicated that when TG2 activity was inhibited by CYS, the expression levels of BMP-2 and VEGF and the osteoblast markers OCN, OPN, and COL I were dramatically decreased in the TG2-EMSC group. These effects might be due to the abrogation of the cross-linking function of TG2 by CYS.

Fig. 9 Evaluation of bone regeneration in SD rat skull bone defect. A 3D CT reconstructions of whole skulls showing the bone defect and the regenerated bone at 1, 4, 8, and 12 weeks after the implantation of the three kinds of grafts in vivo. **B** Analysis of the bone volume/total volume (BV/TV) in the respective groups. **$P < 0.01$; *$P < 0.05$.

Similarly, ALP activity and mineralized nodule formation were also significantly decreased after treatment with CYS. These results demonstrate that TG2 overexpression could substantially promote osteogenic differentiation and maturation, thus suggesting that TG2 might also play an important role in mineralization of the fibrin scaffold, which could transform the fibrin gel into bone-like tissue in vitro before transplantation.
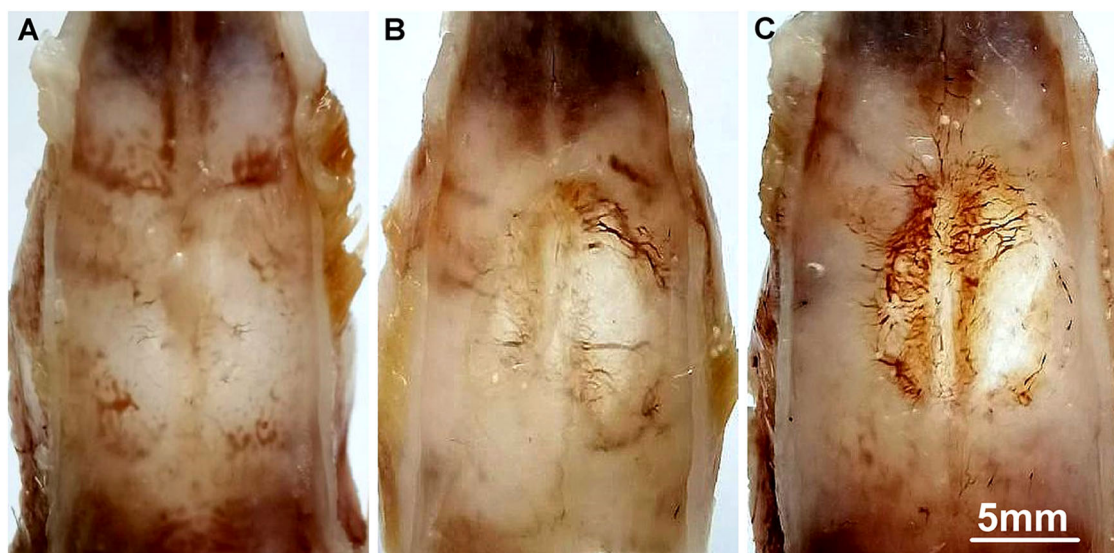
Fig. 10 Gross appearance of the cranial bone at 12 weeks after graft transplantation into the defect. In the TG2-EMSC/fibrin group (**A**), the cranial defect was almost fully repaired by regenerative bone, and the surface of the skull was smooth. In the EMSC/fibrin group (**B**), the cranial defect was partially repaired, and the translucent area of the defect was observed. Fewer regenerative blood vessels were observed in the regenerative tissue in the defect area. In the fibrin group (**C**), almost no repair of the cranial defect was observed, and a large translucent area of the defect was observed. There were many purplish-red regenerative blood vessels radially distributed in the regenerative tissue in the defect area.

To explore whether the fibrin scaffold was an ideal functional biomaterial for bone tissue engineering, an experiment of calcification of the cell-free fibrin scaffold was carried out in vitro. The fibrin scaffold without cells immersed in osteogenic induction medium with additional ALP showed obvious calcification, while little calcium deposition was observed in the fibrin scaffold immersed in osteogenic induction medium without ALP. This finding suggests that ALP plays a key role in fibrin scaffold calcification. These results not only indicate that the fibrin scaffold is an ideal substrate for bone tissue engineering but also suggest that EMSC-derived osteoblasts can enhance fibrin scaffold calcification by sustaining active ALP. In other words, the fibrin scaffolds and EMSCs may complement each other and, together with the intrinsic osteoblasts around the transplantation area in vivo, synergistically promote bone defect repair. In addition, the TG2 secreted by TG2-EMSCs could cross-link the ALP with the fibrin scaffold and both prolong the half-life and preserve the high local concentration of ALP, thereby enhancing calcification of the fibrin scaffold.

Osteoblast differentiation is initially controlled by various morphogens, signaling molecules, and transcriptional regulators. Numerous studies have shown that TGF-β/BMP and Wnt/β-catenin are involved and strongly induce osteoblast differentiation in a variety of stem cell types, including MSCs[33]. The data of this study reveal that EMSCs secrete BMP-2, which belongs to the TGF-β superfamily and acts as a robust osteogenic factor and bone formation stimulator. Surprisingly, BMP-2 staining was diffusely distributed in the EMSCs but clustered in the TG2-EMSCs. This difference in the BMP-2 distribution may be due to the cross-linkage of BMP-2 via TG2. Importantly, Beazley and Nurminskaya[34] reported that BMP-2 retains its biological activity after cross-linking via TG2. In addition, in this study, Western blotting data showed that TG2 gene transfection significantly increased the level of BMP-2. Immunofluorescence staining showed that although the EMSCs synthesized BMP-2, the osteogenic capacity of the EMSCs was weaker than that of the TG2-EMSCs. The secreted BMP-2 may have been rapidly cleared in the EMSC cultures, but immobilized upon cross-linkage with the ECM by TG2, prolonging the half-life and preserving the high local concentration of BMP-2 in the scaffold (graft).

Bone is a highly vascularized connective tissue, and skeletal vasculature plays a significant role in the process of bone development. A high local concentration of VEGF is essential for the coupling of angiogenesis and osteogenesis in vivo. VEGF acts as a chemotactic molecule, attracting endothelial cells to bone tissue and directly controlling the differentiation and functions of osteoblasts and osteoclasts, thereby participating in bone remodeling[35]. The results of this study showed that similar to BMP-2 expression, VEGF expression was significantly increased in TG2-EMSCs, which could promote vascularization of the bone-like graft in vivo.

In addition to seed cells, scaffolds are also indispensable for tissue reconstruction. Tissue-engineered scaffolds should be rationally designed to act as ideal carriers and substrates for seed cell growth and differentiation[36]. Tissue-engineered grafts for the repair of large defects should support osteogenesis, osteoinduction and osteoconduction in vivo. The healing of bone defects is a complex physiological process that involves an orchestrated series of cellular events. As described in our previous study, a fibrin scaffold can provide a suitable microenvironment for bone regeneration that allows cell attachment, proliferation, and differentiation. In addition, the sponge-like structure of the fibrin scaffold was favorable for ECM deposition and graft vascularization in vivo, which are excellent properties for biomaterials used in bone tissue engineering. Engler and Guilak reported that the mechanical properties of the ECM exert a significant influence on the determination of cell fate, which plays a key role in the osteogenic differentiation of stem cells[37,38]. The results of this study show that induced TG2-EMSCs can secrete high levels of ECM/bone matrix components, including LN, FN, COL I, OCN, and OPN, and growth factors, such as VEGF and BMP-2, in vitro. However, to the best of our knowledge, the deposition of free bone-associated protein in bone defects is difficult, and soluble cell growth factors are rapidly consumed in vivo. Increasing evidence has revealed that TG2 is an important extracellular cross-linking enzyme involved in ECM turnover. Thus, we forced EMSCs to overexpress TG2, and these TG2-overexpressing cells were then seeded in the fibrin scaffold. Specifically, TG2 was secreted into the ECM; TG2 has been demonstrated to have a high affinity for FN and promote the adhesion and survival of osteoblasts, BMSCs, and many tumor cells[39]. Moreover, TG2 is a cross-linker of COL I. The cross-linking of COL I by TG2 has been shown to increase the adhesion and differentiation efficiency of human BMSCs without signs of cytotoxicity[40]. Bone matrix proteins, including OPN, bone sialoprotein, and alpha2 HS-glycoprotein, are TG2 substrates, and the covalent cross-linking of these substrates via TG2 plays an important role in bone matrix maturation and calcification[41].

The deposition of abundant ECM and bone-related proteins, such as OCN and OPN, into the TG2-EMSC/fibrin scaffold was observed in vitro. Moreover, bands of proteins of interest with different molecular weights were observed by Western blotting, suggesting that this deposition might be mediated by linking via TG2. These results confirm that soluble cell growth factors were converted to a stable status and were cross-linked with the scaffold and that free bone-associated proteins and ECM components were immobilized, resulting in the formation of a complex network of bone-related proteins, ECM

components, and cell growth factors. The TG2-EMSC/fibrin scaffold complex can biologically be considered an osteoid. This osteoid contained abundant fibrin fibers, ECM components, and cell growth factors secreted by the seed cells that were cross-linked with the fibrin scaffold through TG2. In addition, this osteoid could be regarded as a release system for trophic factors and a 3D scaffold for cell growth and osteogenic differentiation. Finally, this sponge-like scaffold was transformed into bone-like tissue due to mineralization.

This study found that TG2 can promote the osteogenic differentiation of EMSCs in vitro. To determine whether the TG2-EMSC/fibrin scaffold can promote the repair of bone defects in vivo, the TG2-EMSC/fibrin scaffold was first transformed into functional bone-like tissue in vitro and then transplanted into a critical-sized cranial bone defect in a rat model for evaluation of the therapeutic efficacy of the bone-like graft in bone defect repair. As expected, the TG2-EMSCs maintained the differentiated phenotype of osteoblasts/osteocytes and produced bone matrix in the grafts in vivo. Meanwhile, there were densely distributed regenerative blood vessels in the graft, suggesting that the TG2-EMSC/fibrin scaffold (bone-like graft) could be vascularized in vivo. The 3D CT reconstructions of the whole skull and the appearance on gross observation of the cranial bone indicated that transplantation of the engineered bone-like graft, made of TG2-EMSCs and a fibrin scaffold, could promote the healing of critical-sized bone defects. For scaffold implantation in load-bearing bone defects, the scaffold should possess adequate mechanical strength to withstand the mechanical requirements. Thus, the engineered bone-like graft can only be used as a material for bone defect restoration in non-load-bearing bone or in combination with internal fixation.

Conclusions

In summary, in this study, a novel functional tissue-engineered bone-like graft made of TG2 gene-modified EMSCs and a fibrin scaffold was designed and constructed, and the therapeutic efficacy of the bone-like graft in bone defect repair after transplantation was evaluated. The experimental results indicate that the TG2-EMSCs overexpressed TG2, which strongly promoted the osteogenic differentiation of the TG2-EMSCs in the fibrin scaffold in vitro. Moreover, TG2 could enhance the deposition of ECM proteins (i.e., bone matrix) into the scaffold, followed by calcification of the bone matrix and transformation of the scaffold into functional bone-like tissue in vitro. More importantly, after transplantation into critical-sized cranial defects in a rat model, the bone-like graft showed excellent therapeutic efficacy in bone defect repair in vivo.

Author details

[1]Nanjing Gaochun People's Hospital, 211300 Nanjing, People's Republic of China. [2]School of Medicine, Jiangsu University, 212001 Zhenjiang, Jiangsu Province, People's Republic of China. [3]School of Medicine, Jiangnan University, 214122 Wuxi, Jiangsu Province, People's Republic of China. [4]State Key Laboratory of Food Science and Technology, Jiangnan University, 214122 Wuxi, Jiangsu Province, People's Republic of China. [5]Center for Soft Condensed Matter Physics and Interdisciplinary Research, Soochow University, 215006 Suzhou, People's Republic of China

Author contributions

W.S. and N.L. conceived and designed the study. Y.Q., X.Z., L.B., X.Y., X.T., G.Y., Y. D., D.L., S.B., Y.W., W.W., and Z.Z. performed the experiments. W.S. wrote the paper, and Y.W., X.Z., Z.Z., X.L., and N.L. reviewed and edited the manuscript. All authors have read and approved the manuscript.

Data availability

All data generated or analyzed during this study are included in this published article.

Conflict of interest

The authors declare no competing interests.

Publisher's note

Springer Nature remains neutral with regard to jurisdictional claims in published maps and institutional affiliations.

Supplementary information The online version contains supplementary material available at https://doi.org/10.1038/s41427-021-00297-w.

References

1. Fearon, J. A., Griner, D., Ditthakasem, K. & Herbert, M. Autogenous bone reconstruction of large secondary skull defects. *Plast. Reconstruct. Surg.* **139**, 427 (2017).
2. Sagi, H. C., Young, M. L., Gerstenfeld, L., Einhorn, T. A. & Tornetta, P. Qualitative and quantitative differences between bone graft obtained from the medullary canal (with a reamer/irrigator/aspirator) and the iliac crest of the same patient. *J. Bone Jt. Surg. Am.* ume **94**, 2128–2135 (2012).
3. Saeed, H. et al. Mesenchymal stem cells (MSCs) as skeletal therapeutics—an update. *J. Biomed. Sci.* **23**, 1–15 (2016).
4. Sándor, G. K. et al. Adipose stem cells used to reconstruct 13 cases with cranio-maxillofacial hard-tissue defects. *Stem Cells Transl. Med.* **3**, 530–540 (2014).
5. Rinaldo, F. S., Silva, S. G. R. D., Estela, S. C., Jesus, S. E. M. & Sérgio, C. P. Biology of bone tissue: structure, function, and factors that influence bone cells. *Biomed. Res. Int.* **2015**, 421746 (2015).
6. Schmidt, J. R. et al. Sulfated hyaluronic acid and dexamethasone possess a synergistic potential in the differentiation of osteoblasts from human bone marrow stromal cells. *J. Cell. Biochem.* **120**, 8706–8722 (2019).
7. Deng, W. et al. EMSCs build an all-in-one niche via cell–cell lipid raft assembly for promoted neuronal but suppressed astroglial differentiation of neural stem cells. *Adv. Mater.* **31**, 1806861 (2019).
8. Zhijian et al. Nasal ectomesenchymal stem cells: Multi-lineage differentiation and transformation effects on fibrin gels—ScienceDirect. *Biomaterials* **49**, 57–67 (2015).
9. Gao, G. & Cui, X. Three-dimensional bioprinting in tissue engineering and regenerative medicine. *Biotechnol. Lett.* **38**, 203–211 (2016).
10. Melke, J., Midha, S., Ghosh, S., Ito, K. & Hofmann, S. Silk fibroin as biomaterial for bone tissue engineering. *Acta Biomater.* **31**, 1–16 (2016).
11. Alireza, N., Jamal, A. S., Roza, V. G., Ashraf, H. Z. & Webster, T. J. A review of fibrin and fibrin composites for bone tissue engineering. *Int. J. Nanomed.* **12**, 4937–4961 (2017).
12. Wu, X., Ren, J. & Li, J. Fibrin glue as the cell-delivery vehicle for mesenchymal stromal cells in regenerative medicine. *Cytotherapy* **14**, 555–562 (2012).
13. Lv, J. et al. Enhanced angiogenesis and osteogenesis in critical bone defects by the controlled release of BMP-2 and VEGF: implantation of electron beam melting-fabricated porous Ti6Al4V scaffolds incorporating growth factor-doped fibrin glue. *Biomed. Mater.* **10**, 035013 (2015).
14. Anitua, E., Zalduendo, M. M., Prado, R., Alkhraisat, M. H. & Orive, G. Morphogen and proinflammatory cytokine release kinetics from PRGF-Endoret fibrin scaffolds: evaluation of the effect of leukocyte inclusion. *J. Biomed. Mater. Res. Part A* **103**, 1011–1020 (2015).
15. Liu, M. et al. Injectable hydrogels for cartilage and bone tissue engineering. *Bone Res.* **5**, 75–94 (2017).
16. Lichte, P., Pape, H. C., Pufe, T., Kobbe, P. & Fischer, H. Scaffolds for bone healing: concepts, materials and evidence. *Injury* **42**, 569–573 (2011).
17. Belkin, A. M. Extracellular TG2: emerging functions and regulation. *FEBS J.* **278**, 4704–4716 (2011).
18. Wang, Z. & Griffin, M. TG2, a novel extracellular protein with multiple functions. *Amino Acids* **42**, 939–949 (2012).
19. Cavelier, S., Dastjerdi, A. K., McKee, M. D. & Barthelat, F. Bone toughness at the molecular scale: a model for fracture toughness using crosslinked osteopontin on synthetic and biogenic mineral substrates. *Bone* **9**, 19706 (2018).
20. Maria, N. Transglutaminases in mineralized tissues. *Front. Biosci. A* **11**, 1591 (2006).
21. Weisel, J. W. & Litvinov, R. I. In *Fibrous Proteins: Structures and Mechanisms* (eds Squire, J. M. & Parry, D. A. D.) 405–456 (Cham, 2017).
22. Komáromi, I., Bagoly, Z. & Muszbek, L. Factor XIII: novel structural and functional aspects. *J. Thrombosis Haemostasis* **9**, 9–20 (2011).
23. Barsigian, C., Stern, A. M. & Martinez, J. Tissue (type II) transglutaminase covalently incorporates itself, fibrinogen, or fibronectin into high molecular weight complexes on the extracellular surface of isolated hepatocytes. Use of 2-[(2-oxopropyl)thio] imidazolium derivatives as cellular transglutaminase inactivators. *J. Biol. Chem.* **266**, 22501 (1991).
24. Al-Jallad, H. F. et al. Transglutaminase activity regulates osteoblast differentiation and matrix mineralization in MC3T3-E1 osteoblast cultures. *Matrix Biol.* **25**, 135–148 (2006).
25. Ginn, S. L., Amaya, A. K., Alexander, I. E., Edelstein, M. & Abedi, M. R. Gene therapy clinical trials worldwide to 2017: An update. *J. Gene Med.* **20**, e3015 (2018).
26. Crystal, R. G. Adenovirus: the first effective in vivo gene delivery vector. *Hum. Gene Ther.* **25**, 3–11 (2014).
27. Jeitner, T. M., Delikatny, E. J., Ahlqvist, J., Capper, H. & Cooper, A. J. Mechanism for the inhibition of transglutaminase 2 by cystamine. *Biochem. Pharmacol.* **69**, 961–970 (2005).
28. Carrion, B., Janson, I. A., Kong, Y. P. & Putnam, A. J. A safe and efficient method to retrieve mesenchymal stem cells from three-dimensional fibrin gels. *Tissue Eng. Part C* **20**, 252–263 (2014).
29. Cox, D. B. T., Platt, R. J. & Zhang, F. Therapeutic genome editing: prospects and challenges. *Nat. Med.* **21**, 121–131 (2015).
30. Nurminsky, D. et al. Transglutaminase 2 regulates early chondrogenesis and glycosaminoglycan synthesis. *Mech. Dev.* **128**, 234–245 (2011).
31. Li, B., Tian, X., Hu, R., Xu, F. & Zhao, J. Mechanism of BMP and TG2 in mesenchymal stem cell osteogenesis. *Eur. Rev. Med. Pharm. Sci.* **19**, 4214–4219 (2015).
32. Yin, X., Chen, Z., Liu, Z. & Song, C. Tissue transglutaminase (TG2) activity regulates osteoblast differentiation and mineralization in the SAOS-2 cell line. *Braz. J. Med. Biol. Res.* **45**, 693–700 (2012).
33. Wu, M., Chen, G. & Li, Y.-P. TGF-β and BMP signaling in osteoblast, skeletal development, and bone formation, homeostasis and disease. *Bone Res.* **4**, 1–21 (2016).

34. Beazley, K. E. & Nurminskaya, M. BMP2 cross-linked by transglutaminase 2 to collagen-plla scaffold promotes osteogenic differentiation in mesenchymal stem cells. *Biotechnol. Lett.* **36**, 1901–1907 (2014).

35. Filipowska, J., Tomaszewski, K. A., Niedźwiedzki, Ł., Walocha, J. A. & Niedźwiedzki, T. The role of vasculature in bone development, regeneration and proper systemic functioning. *Angiogenesis* **20**, 291–302 (2017).

36. Abdeen, A. A. & Saha, K. Manufacturing cell therapies using engineered biomaterials. *Trends Biotechnol.* **35**, 971–982 (2017).

37. Engler, A. J., Sen, S., Sweeney, H. L. & Discher, D. E. Matrix elasticity directs stem cell lineage specification. *Cell* **126**, 677–689 (2006).

38. Guilak, F. et al. Control of stem cell fate by physical interactions with the extracellular matrix. *Cell Stem Cell* **5**, 17–26 (2009).

39. Soluri, M. F. et al. Mapping the minimum domain of the fibronectin binding site on transglutaminase 2 (TG2) and its importance in mediating signaling, adhesion, and migration in TG2-expressing cells. *FASEB J.* **33**, 2327–2342 (2019).

40. Fortunati, D. et al. of collagen I by tissue transglutaminase provides a promising biomaterial for promoting bone healing. *Amino Acids* **46**, 1751–1761 (2014).

41. Kaartinen, M. T., El-Maadawy, S., Räsänen, N. H. & McKee, M. D. Tissue transglutaminase and its substrates in bone. *J. Bone Miner. Res.* **17**, 2161–2173 (2002).